REPORT DOCUMENTATION PAGE

Form Approved OMB No. 0704-0188

1. AGENCY USE ONLY (*Leave Blank*)	2. REPORT DATE	3. REPORT TYPE AND DATES COVERED
	June 2000	Final Report (01Jun95-01Mar97)

4. TITLE AND SUBTITLE
Transient Transport in Nanostructure Devices Via The Quantum Liouville Equation In The Coordinate Representation

5. FUNDING NUMBERS
C: N00014-95-C-0224

6. AUTHOR(S)
H.L. Grubin

7. PERFORMING ORGANIZATION NAME(S) AND ADDRESS(ES)
Scientific Research Associates, Inc.
30C Hebron Avenue, P.O. Box 1058
Glastonbury, CT 06033

8. PERFORMING ORGANIZATION REPORT NUMBER
R9250F

9. SPONSORING/MONITORING AGENCY NAME(S) AND ADDRESS(ES)
Office of Naval Research
Ballston Tower One
800 North Quincy Street
Arlington, VA 22217-5660

10. SPONSORING/MONITORING AGENCY REPORT NUMBER

11. SUPPLEMENTARY NOTES

12a. DISTRIBUTION/AVAILABILITY STATEMENT
Approved for public release; distribution unlimited.

12b. DISTRIBUTION CODE

13. ABSTRACT (*Maximum 200 words*)

This document summarizes work performed under US Navy, Office of Naval Research Contract: N00014-95-C-0024 to examine transient transport in quantum structures via the quantum Liouville equation in the coordinate representation. For comparison transient results via the Wigner distribution are included. The issue of dissipation in nanostructures was also initiated in this study. A summary of the dissipation results is included in a reprint.

14. SUBJECT TERMS
Transient Transport
Density Matrix
Wigner Functions
Nanostructures
Dissipation

15. NUMBER OF PAGES
23

16. PRICE CODE

17. SECURITY CLASSIFICATION OF REPORT	18. SECURITY CLASSIFICATION OF THIS PAGE	19. SECURITY CLASSIFICATION OF ABSTRACT	20. LIMITATION OF ABSTRACT
UNCLASSIFIED	UNCLASSIFIED	UNCLASSIFIED	UL

Scientific Research Associates, inc.

30C Hebron, P.O. Box 1058
Glastonbury, Connecticut 06033
Tel: (860) 659-0333
Fax: (860) 633-0676

Final Report R9250F

TRANSIENT TRANSPORT IN NANOSTRUCTURE DEVICES VIA THE QUANTUM LIOUVILLE EQUATION IN THE COORDINATE REPRESENTATION

Submitted to
U. S. Navy
Office of Naval Research

800 North Quincy Street
Arlington, Virginia, 22217-5660

June 2000

TRANSIENT TRANSPORT IN NANOSTRUCTURE DEVICES VIA THE QUANTUM LIOUVILLE EQUATION IN THE COORDINATE REPRESENTATION

Table of Contents

TRANSIENT TRANSPORT IN NANOSTRUCTURE DEVICES VIA THE QUANTUM LIOUVILLE EQUATION IN THE COORDINATE REPRESENTATION

Abstract

This document summarizes work performed under US Navy, Office of Naval Research Contract: N00014-95-C-0024 to examine transient transport in quantum structures via the quantum Liouville equation in the coordinate representation. For comparison transient results via the Wigner distribution are included. The issue of dissipation in nanostructures was also initiated in this study. A summary of the dissipation results is included in a reprint.

1. Introduction

In the past decade there have been demonstrations that band structure engineered devices with nanoscale dimensions have the potential of providing a dramatic shift in semiconductor technology. One significant illustration of this is the development of multiple value logic and memory circuits based on utilization of the negative differential resistance properties of either isolated resonant tunneling structures or embedded RTDs (as in the case of resonant tunneling bipolar transistors). Another is the demonstration of the RTD as a high frequency relaxation oscillator, simplifying the prospect of developing high frequency clocks. But, the operation of either logic or memory devices requires knowledge only of the static properties of RTDs, as does the operation of the RTD as a relaxation oscillator.

But as device size shrinks, the active region of the device approaches the size of the electron wave-packet, transit times approach coherence times, and the device operation cannot reliably be treated within a steady state picture. Rather transients are required for a basic understanding of the device operating principles. This study under US Navy, Office of Naval Research Contract: N00014-95-C-0024 was concerned with transient quantum transport. The vehicle for examining transient issues was the density matrix in the coordinate representation. More recent studies have focused on transient transport via the Wigner distribution function.

Transient transport via the quantum Liouville equation in the coordinate representation was begun under this contract. A comparison to the Wigner studies is given below. Unless otherwise noted all transient calculations are coupled to Poisson's equation.

In addition a study of dissipation was initiated. This is summarized in a reprint included with this report.

2. Transient Behavior with the Time Dependent Liouville Equation in the Coordinate Representation (Restricted to the Single Time Representation)

All of the time dependent simulations were in the single time representation. Two time transients were formulated but not implemented. For the single time density operator the quantum Liouville equation is:

$$(1) \qquad i\hbar \frac{d\,\rho_{op}(t)}{dt} = \left[H(t), \rho_{op}(t)\right] + \left[H(t)_{dissipation}, \rho_{op}(t)\right]$$

Here: $\rho_{op}(t)$ is the density operator and $H(t)_{dissipation}$ is that portion of the Hamiltonian describing dissipation.

Under this study the quantum Liouville equation was studied within the coordinate representation. The full coordinate representation is a six dimensional space plus time, where the density matrix is expressed as: $\rho(x, y, z; x', y', z'; t)$. We dealt only with the restricted situation where the carriers are free in two directions, *y and z*. This is equivalent in the Wigner picture to dealing with one-dimensional transport and ignoring any non-parabolic contributions from transverse momentum states.

Dissipation was introduced through quasi-Fermi levels as shown below in equation (2):

$$i\hbar\frac{\partial\rho(x,x',t)}{\partial t}=$$

(2)

$$-\frac{\hbar^2}{2m}\left(\frac{\partial^2}{\partial x^2}-\frac{\partial^2}{\partial x'^2}\right)\rho(x,x',t)+\left[\left(V(x)-V(x')\right)-\left(E_F(x)-E_F(x')\right)\right]\rho(x,x',t)$$

As we are only interested in differences in potential energy, we are only interested in differences in the quasi-Fermi levels. Here:

(3) $$E_F(L)-E_F(0)=-\int_0^L dx\, m\, v(x)\Gamma(x)$$

In the above the velocity $v(x)$, is obtained as the ratio of the position dependent particle current density and the carrier density. $\Gamma(x)$ is a position dependent scattering rate. The particle current density is given by the diagonal component of the current-density-operator in the coordinate representation:

(4) $$J(x,x',t)=\frac{\hbar}{2mi}\left(\frac{\partial}{\partial x}-\frac{\partial}{\partial x'}\right)\rho(x,x',t)\quad(4)$$

The quasi-Fermi energy was computed subject to the constraint that the kinetic energy of entering and exiting carriers are equal. (The quasi-Fermi level approach to dissipation was examined in detail in a variety of circumstances. In particular, under conditions appropriate to classical transport, all of the standard results were obtained. In particular, Ohm's law was retrieved. Under conditions appropriate to quantum corrections this dissipation model appears to provide reasonable current-voltage characteristics.)

In all transient calculations, those via the density matrix in the coordinate representation and those via the Wigner representation, total current included both *displacement and particle conduction* contributions; the former proportional to the time derivative of the local electric field. Thus accurate solutions to Poisson's equation were needed.

The boundary conditions on equation (2) incorporated the density matrix equivalent of a displaced Fermi-Dirac distribution. As discussed in the first reprint, the upstream boundary condition is $\rho(x,x')\exp[i(x-x')mJ/(\rho_0\hbar)]$ where $\rho(x,x')$ is the zero current quantum distribution function on the boundary, ρ_0 is the density on the boundary, and J is the current density at the boundary. This condition is also imposed for the time dependent studies. This condition is equivalent to imposing displaced Fermi-Dirac conditions. In the Wigner function calculations, displaced Fermi conditions were not imposed. Rather the normal spatial derivative was set to zero. In both the density matrix and Wigner function calculations, the boundary conditions chosen were designed to provide flat band conditions.

3. Results with the Density Matrix in the Coordinate Representation

For the problems discussed below with the potential energy at the emitter set to zero, the system is brought to steady state for a given collector potential energy. A step change to a new constant value is introduced for $V(L)$, and the resulting time dependent behavior is computed at fixed increments in time. All calculations assumed Fermi statistics, parameters appropriate to GaAs, except for the barriers, and a constant effective mass. For each study a steady state was reached at a value of 100 meV. A step change in voltage to 150 meV was then applied.

Several structures were studied, all 120nm in length. This device length is too small for the requirements of flat band at the boundaries to be met. The choice was based on achieving small time steps and these calculations did indicate a capability to perform transient studies. The transient studies included:

(1) An $N^+N^-N^+$ triple barrier 200 meV structure;
(2) An $N^+N^-N^+$, 300 meV double barrier structure, and
(3) A uniform N-type 300 meV double barrier structure.

The background doping and structure of the double and triple barrier results are shown in figure 1. The results for the triple barrier structure are discussed first.

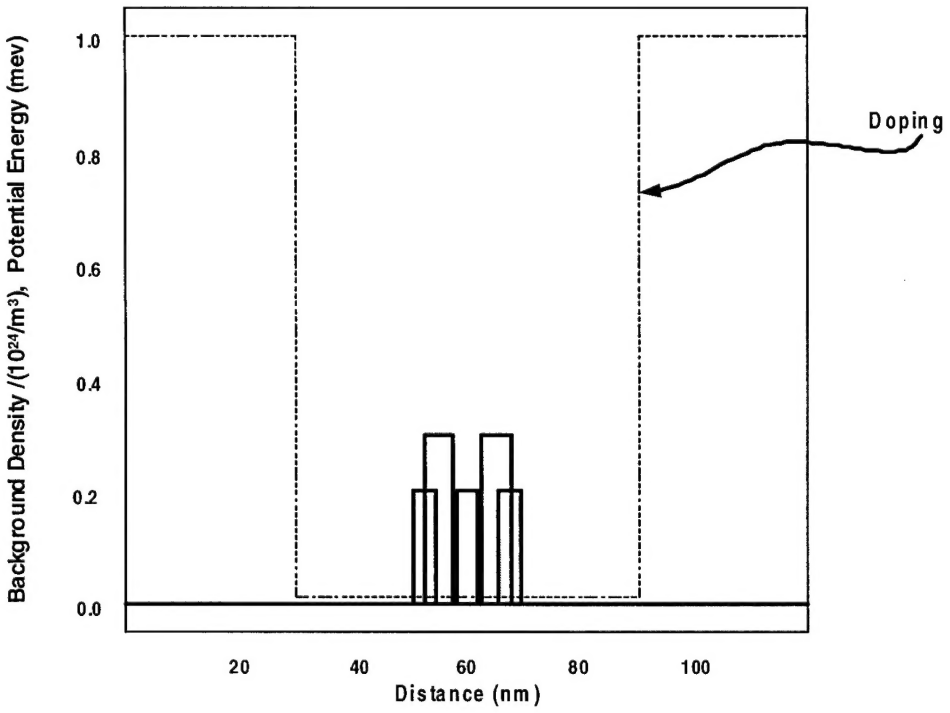

Figure 1: Background doping distribution and the double and triple barrier structures for the transient calculations with the density matrix in the coordinate representation.

The triple barrier structure: At 100 meV the steady state current was $1.477\times10^9 amps/m^2$. Increasing the bias to 150 meV yielded an increased steady state value of current equal to $2.657\times10^9 amps/m^2$. Due to time limitations transitions to lower current with increased bias were not obtained during this transient study. They awaited the more recent Wigner calculation, which is discussed below. The time dependent space charge distribution following the step from 100 meV to 150 meV was followed through a time of 420 fs. The time step was 70fs, and the transient current at the end of each time increment is shown in figure 2. While we did not

carry this calculation to very long times, the initial structure in the calculation shows a period of near 200 fs. This number is significant, as we see very similar structure in transients associated with double barrier structures obtained with the Wigner formulation.

Examining the space charge distribution following the step change in voltage, we found for the cladding regions surrounding the barriers, little difference in density at the different bias levels. Since there are changes in voltage in the surrounding regions, the dominant time dependent behavior is likely due to displacement current contributions. The situation is different in the interior.

Figure 3 displays, for the central 20 nm region the initial steady state solution, the final steady state solution, and for two early time intervals. Several points are noted.

(1) The lowest values of charge density occur within the barriers, and there are three barriers. (This results is expected.)

(2) There is charge accumulation within the two quantum wells. With the greatest amount in the quantum well closest to the emitter contact.

(3) ***The maximum change in the charge distribution within the two quantum wells appears to have occurred within the first 70 fs time step.*** It is within the quantum wells that the peak carrier density occurs. The situation within the barriers is different. Here there is considerable transient behavior with the density not quite reaching its steady state value. The results suggest distributive behavior during the initial transient. Distributive behavior means that within the barriers where there is considerable temporal variation in the charge distribution, we may be seeing a transient inductive contribution to the potential drop in the device. In the quantum wells we may be seeing a capacitive contribution.

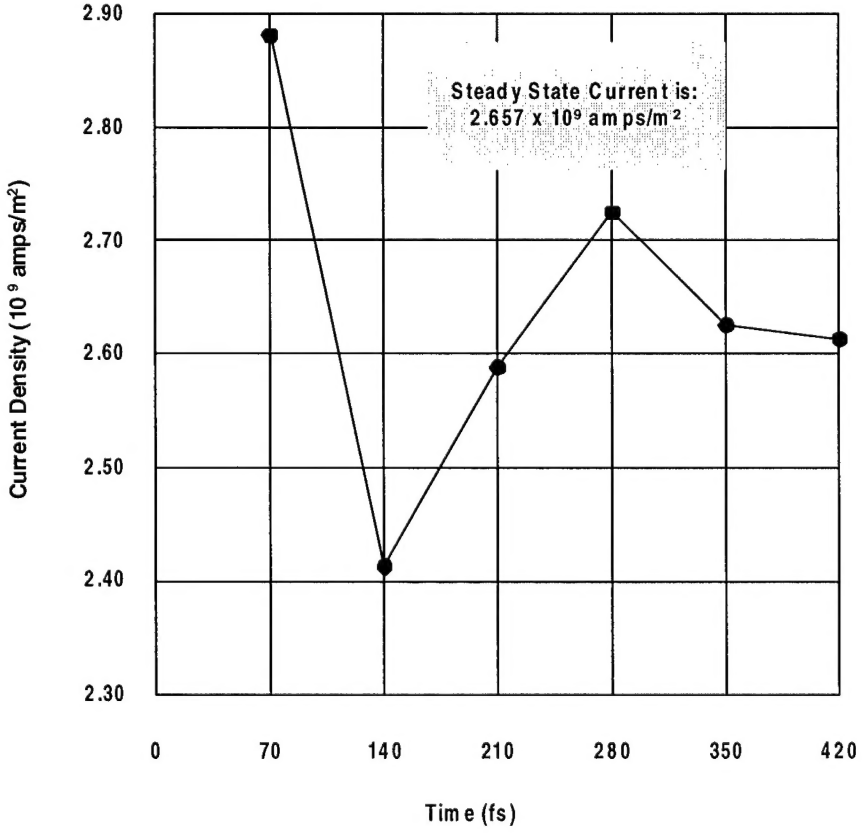

Figure 2: The current transient for the triple barrier structure.

The last point is a new and unexpected result, and bears careful study in the Wigner formulation. From a device operational point of view this means that most of the longer time current transients within the quantum well arise from displacement current contributions. ***It also indicates that there is considerable physics in the sub 70 fs time scale.***

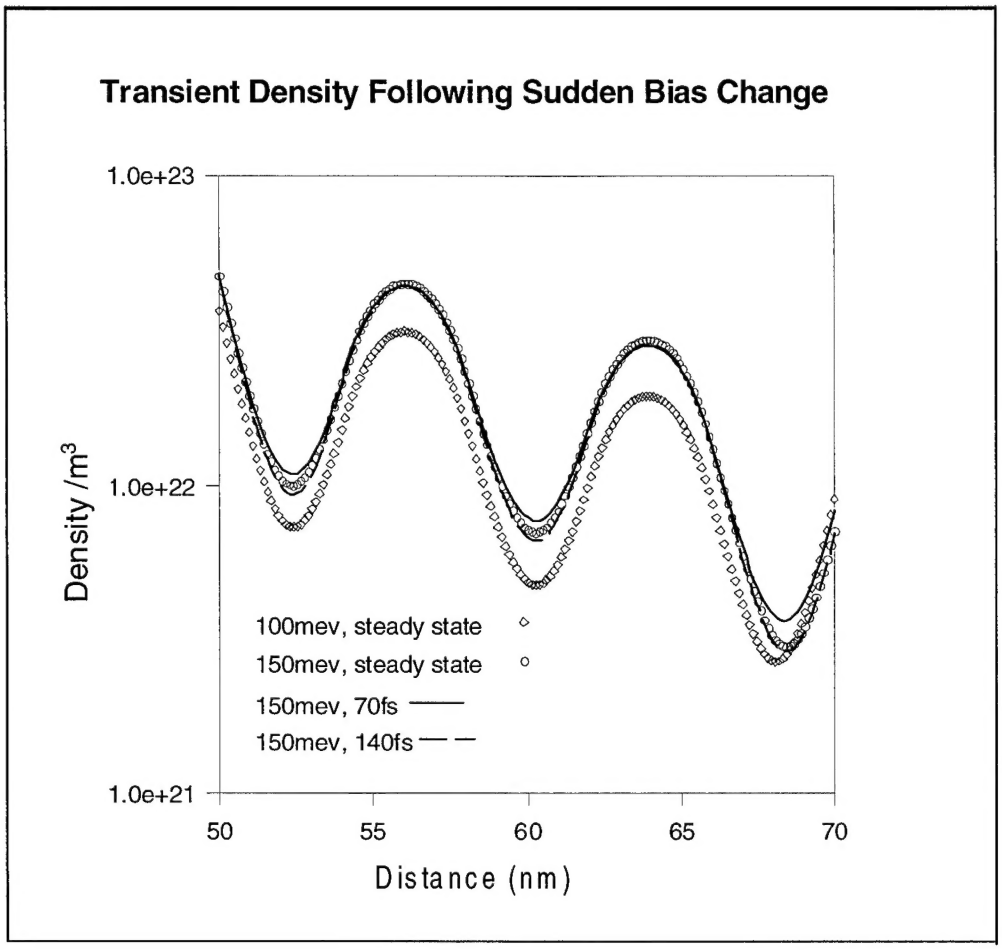

Figure 3: The transient density for the triple barrier structure following a sudden change in bias.

The Double Barrier Structure: The situation for the $N^+N^-N^+$ double barrier structure is similar. Here at a bias of 100 meV, the steady state current is 6.102 x 10^8 amps/m^2, at 150 meV the current is 1.047 x 10^9 amps/m^2. The transient density distribution shows considerably more structure in the cladding regions, than for the triple barrier structure and suggests that conduction current contributions as well as displacement current contributions are significant. The situation in the interior is displayed in figure 4 and is very similar to that of the triple barrier structure. Application of the sudden change in bias results in an increase in charge everywhere within the structure. But here the transient behavior is more dramatic than that arising in the triple barrier struc-

ture. First we see similar behavior in the quantum well, where the carrier density appears to approach its steady state value in a time less than 70fs. The transient behavior associated with the barriers is much different. As in the case of the triple barrier structure where most of the time dependent variation in charge occurred within the barriers, here the time variation in charge density in the barriers is extreme. The consequence of the barrier charge distribution needs to be examined.

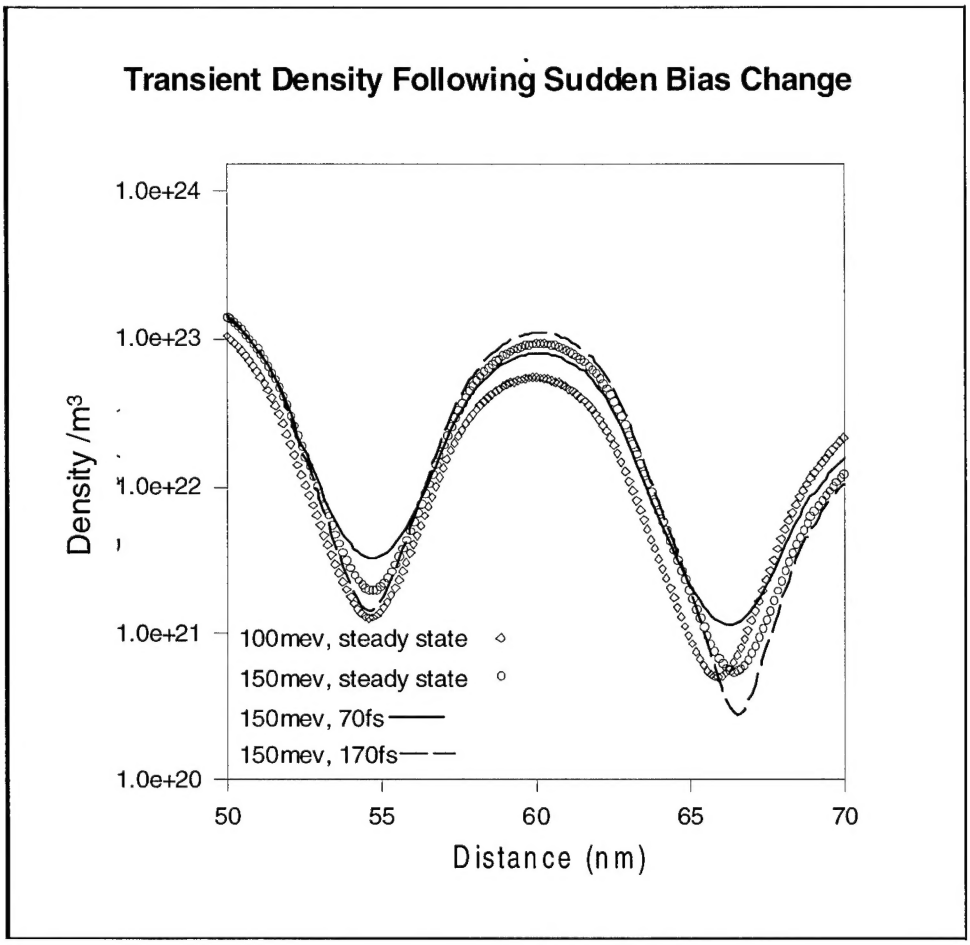

Figure 4: The transient density for the double barrier structure following a sudden change in bias.

***The Uniformly Doped Double Barrier Structure*:** The situation for the double barrier structure embedded in a uniformly doped $10^{24}/m^3$ region also shows time dependent behavior, but the initial and final state distributions of charge are not significantly different, and the steady state distribution of charge appears to be reached in the early time stages. It appears that dielectric relaxation may be playing a significant role here.

4. Transients Via the Wigner Distribution-A Comparison

The detailed charge distribution associated with barriers is far richer than we would expect from simple time independent arguments. More recent work with a Wigner transient algorithm developed at SRA indicates some unusual features; unusual in the sense that they are unlikely to predicted from a simple analysis of the initial and final states. We show these results below.

The calculations were for a resonant tunneling diode with 250 meV barriers, 5 nm wide, and with a 5 nm wide separation. The current voltage characteristics demonstrated a current drop back with no dc hysteresis. The device was subjected to a transient voltage pulse and allowed to settle into equilibrium. The voltage pulse started from approximately 230 meV, a value below the threshold voltage for negative differential conductivity, to approximately 310 meV. The time dependence of the charge distribution is shown in figure 5. Figure 5 is a display of the one-dimensional distribution of charge at different instants of time. The structure is 200 nm long.

We know from the static calculations that the distribution of charge prior to switching to the low current state consists of considerable charge accumulation in the quantum well. After the transition to the low current state there is significant loss of charge within the quantum well, with a large increase in charge on the emitter side of the barrier. The time dependent behavior displayed in figure 5 is consistent with this result. But there is more. It appears that the transition to the high/low charge distribution within the quantum well occurs early in the transient. If this is the case what is the origin on the high frequency current transients that commonly accompany the switching transient? (We note that we have also seen these transients in the density matrix simulations.) A careful look at the simulations indicates that the charge distribution on the emitter side of the barrier is undergoing considerable oscillation, more than that within the quantum well. While the distribution on the emitter side of the barriers affects the charge distribution within the quantum well, the time dependence appears to be dominated by the charge on the emitter side of the barrier.

The time dependence of the charge on the emitter side of the barrier is somewhat obscured in figure 5. In figure 6, we have taken out the transient further (in time), but have broken up the plot into two sections: an early and late time transient. There is considerably more quantum well charge during the initial transient. Note the large charge excursions on the emitter side of the barrier. (The emitter is on the right hand side of both figures.)

The conclusion of the Wigner transients and the density matrix transients is that the structure of the transient oscillation will also depend upon the design of the regions outside of the quantum well.

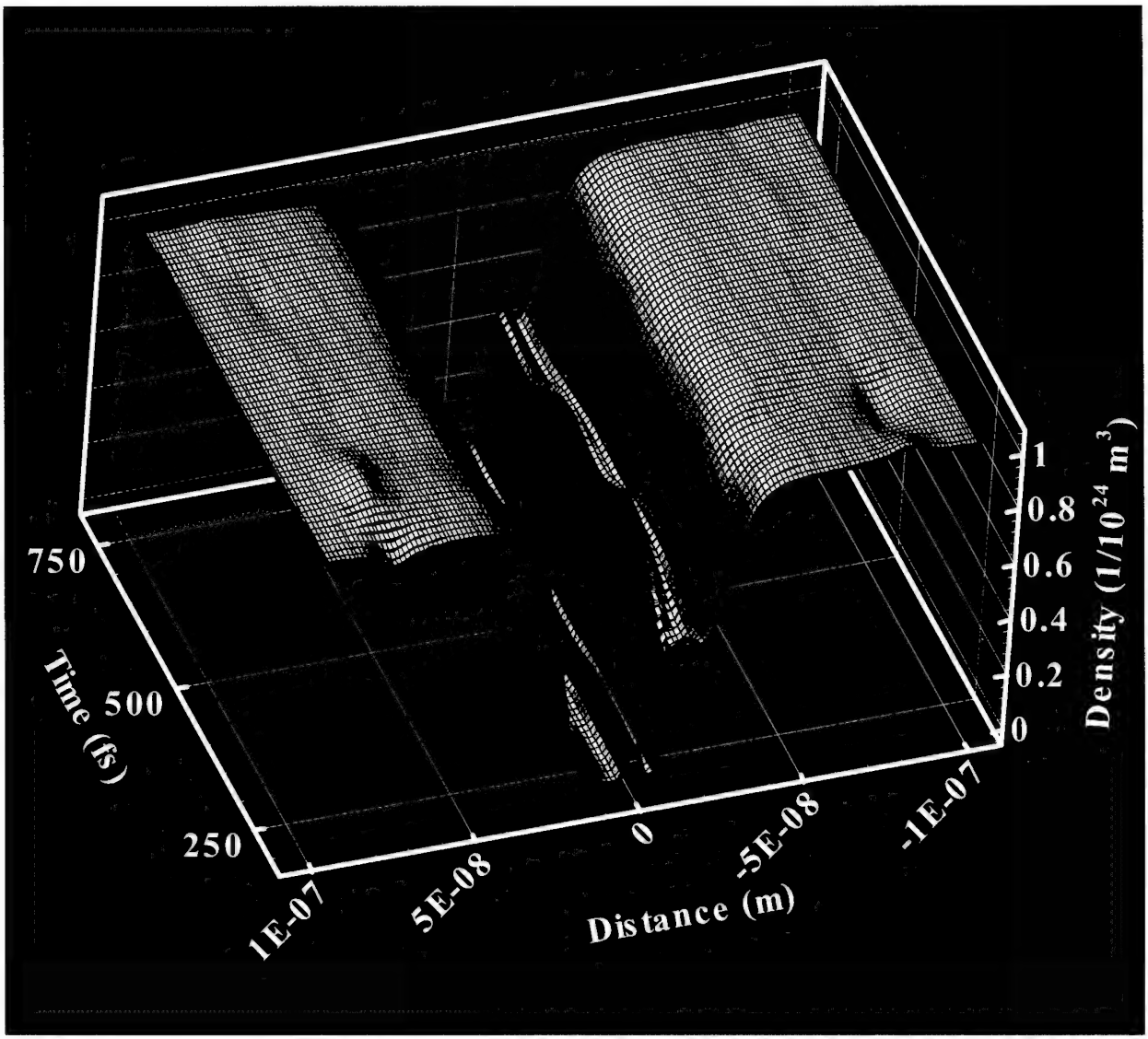

Figure 5: Wigner function calculation of the transient density vs. distance vs. time for a resonant tunneling diode subject to a sudden change in bias.

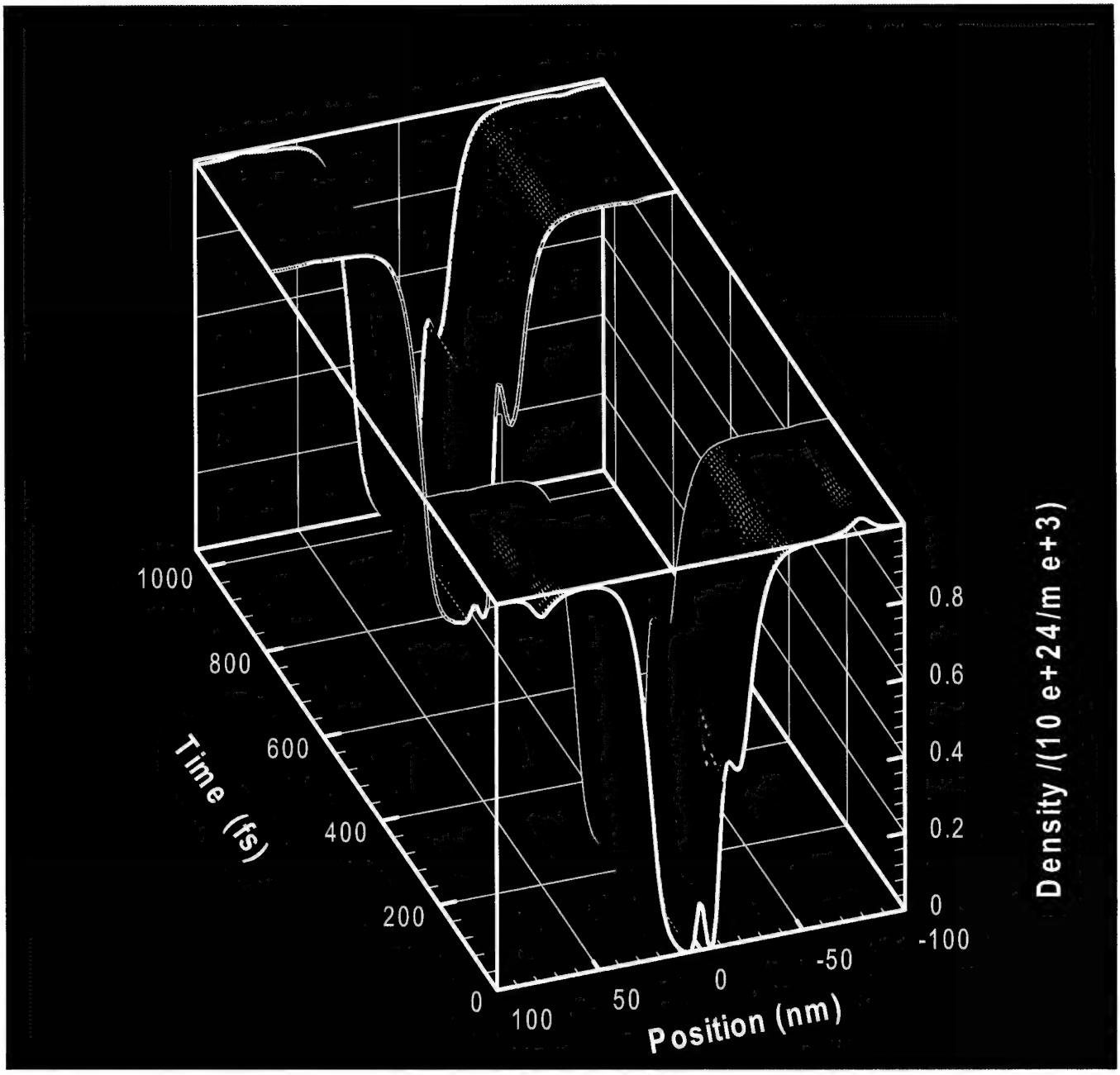

Figure 6: As in figure 5, with two exceptions. Transient is carried out for a longer period of time, and the display is for the initial and final sections of the transient.

5. Summary and Publications

The calculations discussed here demonstrate the richness of the transient phenomena. There is tunneling through a barrier and into the quantum well, coupled to displacement current

effects, and contributions arising due to the magnitude of the density within the structure. We have not attempted to extract a tunneling time from these studies. In actual device studies the tunneling times would be dressed by dielectric contributions and the variability of the self-consistent field. Furthermore, large signal transients would dominate indicating that tunneling times would depend on the initial and final states of the system. The details of the result will also depend upon the scattering parameters.

The transient density matrix study was summarized in a paper that is included with this report (Reprint 1).

As indicated in the introduction there was also a new formulation of dissipation. This is included as Reprint 2.

Reprint 1

SELF-CONSISTENT TIME DEPENDENT SOLUTIONS TO THE QUANTUM LIOUVILLE EQUATION IN THE COORDINATE REPRESENTATION: APPLICATION TO BARRIER STRUCTURES: *Appearing in* ***Hot Carriers in Semiconductors,*** *K. Hess, J. Leburton, U. Ravaioli, eds Plenum Press, NY Page 421 (1995).*

SELF-CONSISTENT TIME DEPENDENT SOLUTIONS TO THE QUANTUM LIOUVILLE EQUATION IN THE COORDINATE REPRESENTATION: APPLICATION TO BARRIER STRUCTURES*

H. L. Grubin[1] , T. R. Govindan[1] , and D. K. Ferry[2]

[1]Scientific Research Associates, Inc.; Glastonbury, Connecticut, USA
[2]Arizona State University; Tempe, AZ, USA

INTRODUCTION

We report on *transient accurate* self-consistent solutions of the quantum Liouville equation in the coordinate representation:

$$i\hbar\frac{\partial\rho(x,x',t)}{\partial t}=-\frac{\hbar^2}{2m}\left(\frac{\partial^2}{\partial x^2}-\frac{\partial^2}{\partial x'^2}\right)\rho(x,x',t)+\left[\left(V(x)-V(x')\right)-\left(E_F(x)-E_F(x')\right)\right]\rho(x,x',t)$$

where $E_F(x)$ and $E_F(x')$ represent quasi-Fermi levels subject to the constraint that the kinetic energy of entering and exiting carriers are equal [Grubin (1995)]. Dissipation is included and current, J_{Total} , contains both *displacement and conduction* contributions. Under time independent conditions the conduction current, j, for a scattering rate Γ satisfies the condition that: $E_F(L)-E_F(0)=-j\int_0^L dx m\Gamma(x)/\rho(x)$. The boundary conditions incorporate current via the density matrix equivalent of a displaced Fermi-Dirac distribution [Grubin *et al.* (1993)].

For this discussion, *V(x=0)=0*, and for a given downstream potential energy *V(L),* the system is brought to steady state. A step change to a new constant value is introduced for *V(L)*, and the resulting time dependent behavior is computed at fixed increments in time.

THE RESULTS

Three symmetric 120 nm length structures were studied: (i) $N^+N^-N^+$ [$N^+=10^{24}/m^3$ (30 nm long), $N^-=10^{22}/m^3$ (30 nm long)], three 200 meV barriers [4 nm barriers, 4 nm wells]; (ii) $N^+N^-N^+$, two 300 meV barriers [5nm barriers, 6 nm well] and (iii) as (ii) but uniformly doped with N

$=10^{24}/m^3$. We assumed Fermi statistics, parameters appropriate to GaAs, except for the barriers, and a constant effective mass. While the length of the structure is too small for any real device studies, the choice achieved small time steps. A step change in voltage to 150 meV from a steady state of 100 meV, was applied.

The triple barrier structure: At 100 meV the steady state current was 1.477 x 10^9 amps/m^2 . At 150 meV steady state yielded a current value of 2.657 x 10^9 amps/m^2. The time dependent space charge distribution following the voltage change was followed through 420 fs. The time step was 70fs, and the transient current at the end of each time increment is shown in figure 1. 70 fs after application of the step change in voltage the charge is generally increased everywhere within the structure. (This is true for the double barrier structure as well.) ***For the regions surrounding the barriers*** we find little time variation in density although the cladding region voltage undergoes changes, suggesting that the dominant time dependent behavior in the cladding region is due to displacement current contributions. ***For the barrier region,*** matters are different; the time dependent changes in voltage are reduced. At 70 fs after application of the voltage step the charge within the barriers exceeds that of the lower bias steady state; see figure 2, which displays denstiy, within the central 20 nm region. At 140 fs there is a decrease in charge within the three barriers and a corresponding increase in charge between the barriers. These results are consistent with an interpretation that a fraction of the charge present at 70 fs has tunneled through the barriers at 140 fs. Excess charge in the wells would subsequently tunnel back toward the respective barriers at a later time, etc., until a steady state is reached.

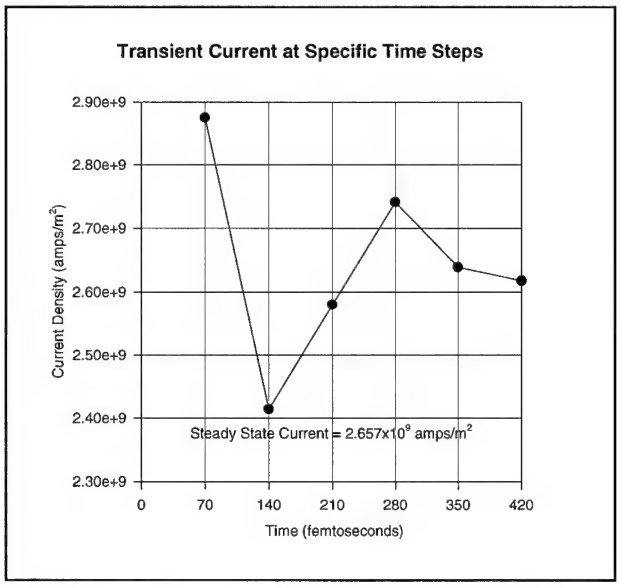

Figure1. Current transient for the triple barrier structure.

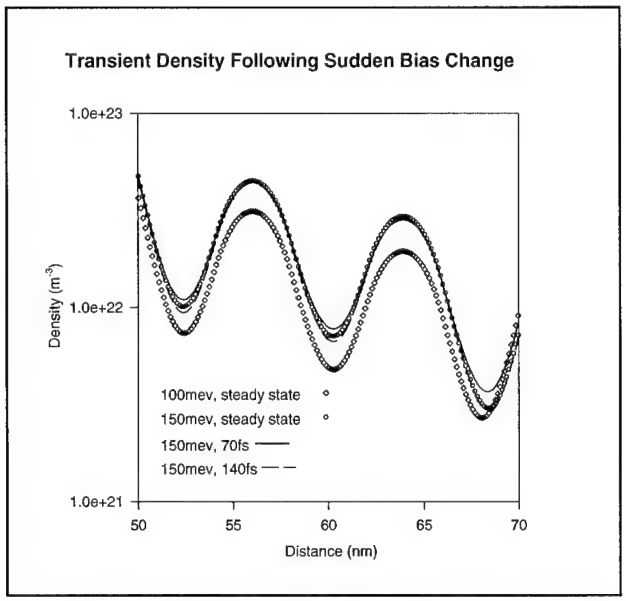

Figure 2. Transient space charge distribution for the triple barrier struture.

The Double Barrier Structures: The situation for the $N^+N^-N^+$ double barrier structure is similar. Here at a bias of 100 meV, the steady state current is 6.102 x 10^8 amps/m^2, at 150 meV the current is 1.047 x 10^9 amps/m^2. ***For the regions surrounding the barriers,*** the transient density distribution shows considerably more structure in the cladding regions than for the triple barrier structure and suggests that conduction current contributions as well as displacement current contributions are significant. ***For the barrier region***, figure 3, charge appears to tunnel to the center well, where the peak density exceeds its steady state value. Tunneling out of this region increases the charge in the barrier. This tunneling into and out of the quantum well may be driving the time dependence of the device.

The situation for the double barrier structure embedded in a uniformly doped $10^{24}/m^3$ region also shows time dependent behavior, but the initial and final state disributions of charge are not significantly different, and the steady state distibution of charge appears to be reached in the early time stages. Dielectric relaxation may be playing a significant role.

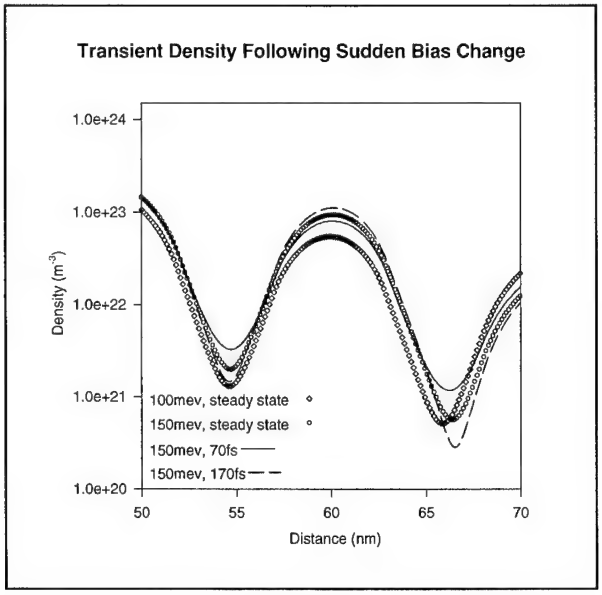

Figure3. Transient space charge distribution for the double barrier structure.

SUMMARY AND REMARKS

The calculations discussed here demonstrate the richness of the transient phenomena. There is tunneling through a barrier and into the quantum well, coupled to displacement current effects, and contributions arising due to the magnitude of the density within the structure. We have not attempted to extract a tunneling time from these studies; in actual device studies, the tunneling times would be dressed by dielectric contributions and the variability of the self consistent field. In most of the calculations the current reaches its steady state value at approximately 500 fs, but weak oscillations beyond this are expected. We have not carried this further. The details of the result will be depend upon the scattering parameters.

ACKNOWLEDGEMENTS

* Supported by ONR

REFERENCES

Grubin, H. L., Govindan, T. R, Kreskovsky, J..P. and Stroscio, M.A., 1993, *Sol. State Electron.* 36:1697

Grubin, H. L. 1995 in "Quantum Transport in Ultrasmall Devices" Eds. D K. Ferry, H. L. Grubin, C. Jacaboni and A. Jauho, Plenum, New York.

Reprint 2

DISSIPATION AND QUANTUM TRANSPORT SIMULATIONS IN NANOSCALE DEVICES: *Appearing in Superlattices and Microstructures* ***20****, 531 (1996).*

Superlattices and Microstructures, Vol. 20, No. 4, 1996

Dissipation and quantum transport simulations in nanoscale devices

H. L. GRUBIN

Scientific Research Associates, Inc., P.O. Box 1058, Glastonbury, CT 06033-6058, U.S.A.

D. K. FERRY, R. AKIS

Department of Electrical Engineering, Arizona State University, Tempe, AZ 85287-5706, U.S.A.

(Received 20 May 1996)

A key simulation issue is the development of a dissipation formalism for the time dependent density operator equation, that is amenable to numerical methods and incorporates the role of the environment on state renormalization and dissipation. Using standard super-operator calculus, projection operators, and separating the system of interest from the reservoir, the relevant operator equation is derived. In addition, the role of the reservoir on renormalizing the energy spectrum is discussed.

Key words: dissipation, quantum transport, Liouville operator.

1. Introduction

Numerical simulation of quantum structures has been a major element of device physics studies. A key issue in these simulations is the development of a formulation for dissipation within the framework of the quantum Liouville equation. Such a formulation is considered below with the discussion based upon Haken [1] for a quantum system (e.g. electrons), which may be far from equilibrium. The system of interest, denoted by S, is kept far from equilibrium by coupling it to other systems with which it exchanges energy. The discussion below is concerned with coupling to a reservoir, denoted by R, whose detailed properties are often of interest.

The quantum Liouville equation for the total system, S plus R is:

$$i\hbar\frac{\partial\rho_T}{\partial t} = [H, \rho_T] \equiv \hat{H}\rho_T, \tag{1}$$

where the 'carat' over the operator, designates a super-operator, as reviewed in Ref. [2]. The super-operator here, also called the Liouville operator, is a commutator-generating super-operator, whose use simplifies the algebra associated with separating the reservoir and system. We use super-operator algebra to obtain a quantum Liouville equation for the reduced density operator for the system S, defined as the trace over the eigenstates of the reservoir, $\rho_s = \mathrm{Tr}^{(R)}\,\rho_T$, (with a similar definition for the reduced density operator for the reservoir, $\rho_R = \mathrm{Tr}^{(S)}\,\rho_T$).

With H_S, H_R, and H_{SR} denoting, respectively, the Hamiltonian of S, R, and the interaction, the Liouville equations for $\rho_S = \mathrm{Tr}^{(R)}\,\rho_T$ and $\rho_R = \mathrm{Tr}^{(S)}\,\rho_T$ are, respectively:

$$i\hbar\frac{\partial\rho_S}{\partial t} = [H_S, \rho_S] + \mathrm{Tr}^{(R)}[H_{SR}, \rho_T], \tag{2}$$

0749–6036/96/080531 + 04 $25.00/0

$$i\hbar\frac{\partial\rho_R}{\partial t} = [H_R, \rho_R] + \mathrm{Tr}^{(S)}[H_{SR}, \rho_T]. \tag{3}$$

The presence in eqs (2) and (3) of the trace over ρ_T means that we do not have a prescription for obtaining an equation for the reduced density operator. We deal with this below. Our approach, which is based upon the projection operators of Mori [3], allows for a general decomposition of the system and reservoir even when they are significantly *entangled*, as is often the case for far-from-equilibrium situations.

2. Projection operators and the time dependent Liouville equation

Starting from equation (1), we consider the projection operator P and its complement Q, such that: $P+Q = 1$. The operator P is chosen such that: $P\rho_T = R\,\mathrm{Tr}^{(R)}\,\rho_T = R\rho_S$, $\mathrm{Tr}^{(R)}\,R = 1$, $PR = R$, where R is chosen to represent the uncoupled distribution of the reservoir, e.g. $R \to f_R = \exp[-\beta H_R]/\,\mathrm{Tr}^{(R)}\{\exp[-\beta H_R]\}$. Thus the effect of the operator P is to take the density (or other) operator, *average over all the non-equilibrium coordinates of the reservoir*, and generate a density operator that is a product of the *equilibrium* reservoir operator and the reduced density operator of the system [4]. The dimension of the subsequent operator is the same as that of ρ_T. It is easy to demonstrate that $P^2 = P$, and that P is a proper projection operator. Then, starting from eqn (1), and after some super-operator algebra, the time dependent Liouville equation becomes:

$$\begin{aligned} i\hbar\frac{\partial\rho_S}{\partial t} &= \hat{H}_S\rho_S + \hat{\tilde{H}}_{RS}\rho_S - \frac{i}{\hbar}\,\mathrm{Tr}^{(R)}\,\hat{H}_{RS}(t)\int_0^t d\tau U(t,\tau)\hat{H}_{RS}(\tau)R\rho_S(\tau) \\ &\quad + \frac{i}{\hbar}\,\mathrm{Tr}^{(R)}\,\hat{H}_{RS}(t)\int_0^t d\tau(PU(t,\tau)\hat{H}_{RS}(\tau)R\rho_S(\tau)) \\ &\quad + \frac{1}{\hbar^2}\,\mathrm{Tr}^{(R)}\,\hat{H}_{RS}(t)\int_0^t d\tau\left(Q\int_\tau^t d\tau' U(t,\tau')P\hat{H}(\tau')V(\tau',\tau)\hat{H}_{RS}(\tau)R\rho_S(\tau)\right). \end{aligned} \tag{4}$$

Here,

$$\tilde{H}_{RS} = \mathrm{Tr}^{(R)}(H_{RS}R), \tag{5}$$

$$V(t,\tau) = \exp-\frac{i}{\hbar}\int_\tau^t d\tau'\hat{H}(\tau')Q, \tag{6}$$

$$U(t,\tau) = \exp-\frac{i}{\hbar}\int_\tau^t d\tau'\hat{H}(\tau'). \tag{7}$$

In eqn (4), all terms are expressed as functions of the reduced density matrix whose time dependence implicitly includes that of the reservoir. The equilibrium reservoir coordinate appears to first order in the second term, *and at least to second order in the remaining terms* (on the right-hand side of eqn (4)). The intra-collisional field effect, for example, arises from the presence of the total Hamiltonian in the exponential of the operator $U(t,\tau)$. Below we introduce approximations to place the above results in perspective. We have also assumed that at $t = 0$, when the interaction is initiated, the density operator is separable into orthogonal operators for the system and the reservoir. In this case, the time dependence of eqn (4) is unaffected by the initial condition.

The last three terms on the right-hand side of eqn (4) represent the effect of *scattering* by the fluctuations in the reservoir. These terms all contribute to an equivalent *self energy*. On the other hand, the second term on the right-hand side is a non-dissipative correction to the system that arises from merely opening the system. Traditionally, this term leads simply to a modification of the eigenvalue spectrum within the system. However, the nature of $\hat{\tilde{H}}_{RS}$ can dramatically affect the entire structure of ρ_S. We examine a test case in the next section.

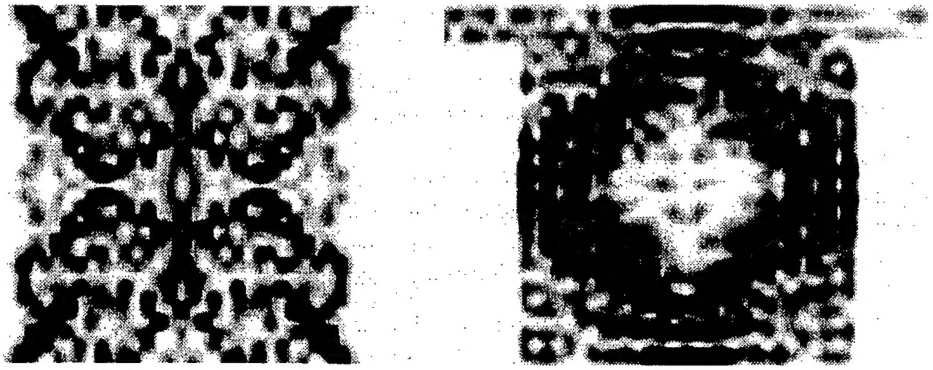

Fig. 1. Plot of the diagonal elements of the density matrix, i.e. the square of the magnitude of the wave function, for a square quantum dot subject to different reservoir couplings. A, The coupling is through tunneling barriers. B, The coupling is via conducting wave guides supporting two modes. Clearly the nature of the coupling creates a different density matrix for the system.

3. Open systems near equilibrium

We consider a square quantum dot that is coupled to the reservoirs through point contacts (these are observable in figure 1B). if the quantum point contacts are closed down to create tunneling barriers (the weak coupling limit), then the properties are quite uniform across the dot. In figure 1A, the diagonal terms of the density matrix in the coordinate representation, $\rho_S(x, y; xy) = |\psi(x, y)|^2$, are presented for the tunneling barrier case. If we vary an applied magnetic field, the transmission function exhibits a series of sharp tunneling peaks.

In contrast, if the point contacts are opened, then entering particles form a collimated beam, which excites a particular set of eigenstates required to reproduce the semi-classical orbits [5]. The excitation is not limited to a single eigenstate, but excites a specific set of modes [6]. It is clear, by comparing Fig. 1A and 1B, the actual values of ρ_S are dramatically affected by the specific details of the interaction with the reservoir.

Another important point is that the energy level shifts and coupling that occur by opening the system to the reservoir are distinctly different from the scattering properties, which lead to level broadening. The former arise from the second term on the right of eqn (4), while the latter arises from the last three terms on the right of eqn (4). Scattering from the reservoir can either cause broadening of the levels, or actually work to stabilize the regular orbits [7]. It might be expected that the latter case would actually lead to narrowing of discrete energy levels.

4. Scattering in non-equilibrium systems

More generally, what is done with eqn (4) depends upon the problem of interest. For the case where the H_{RS} is linear in the momentum [8], the dissipation may be expressed in terms of a quasi-Fermi energy model [9]. Ahn [10] treated the reservoir as stochastic, performed a time average on eqn (4), and obtained a quantum kinetic equation for interacting electron and hole pairs. Krech *et al.* [11] developed a master equation to study macroscopic quantum tunneling of charge in ultra-small single electron tunneling double junctions.

We shall consider some of the more general features of this equation. The third term, which was obtained without the use of perturbation theory, includes the intracollisional field effect. If the off-diagonal elements of the density operator in the momentum representation are taken as small compared to the diagonal elements, we obtain the quantum kinetic equation discussed by Ferry [2], as well as that of Kreiger and Iafrate [12]. This

third term incorporates energy conservation, but only within the system S. We note that the results of Ref. [12] were obtained through perturbation theory with the interaction Hamiltonian as the perturbation estimate. The results here are not totally dependent upon approximations, and suggest a broader applicability of the results of Ref. [12]. Higher-order terms corresponding to the detailed role of the reservoir are readily accessible. These will be discussed in more detail elsewhere.

Acknowledgement—This study was supported by ONR and ARPA.

References

[1] H. Haken. Rev. Mod. Phys. **47**, 67 (1975).
[2] D. K. Ferry, *Semiconductors*, Macmillan Publishing Company, NY (1991).
[3] H. Mori, Prog. Theor. Phys. **33**, 423 (1965); R. W. Zwanzig, in *Lectures in Theoretical Physics*, Edited by W. E. Brittin, B. W. Downs and J. Downs, Interscience, New York: p. 106 (1961).
[4] A similar approach has been used to project a many-particle distribution onto an effective one-electron distribution function by J. Zimmermann, P. Lugli, and D. K. Ferry, Sol. State Electron. **26**, 233 (1983).
[5] R. Akis, D. K. Ferry and J. P. Bird, Superlatt. Microstructures, to be published (1996).
[6] L. A. Wu, Phys. Rev. **A53**, 2053 (1996).
[7] B. S. Helmkamp and D. A. Browne, Phys. Rev. Lett. **76**, 3691 (1996).
[8] I. R. Senitzky, Phys. Rev. **119**, 670 (1960).
[9] H. L. Grubin, T. R. Govindan and D. K. Ferry, *Proc. Ninth Hot Carriers in Semiconductors*. Edited by K. Hess, J.-P. Leburton and U Ravaioli, Plenum Press, New York: p. 421 (1996).
[10] D. Ahn, Phys. Rev. **B50**, 8310 (1994).
[11] W. Krech, A. Hadicke and F. Seume, Phys. Rev. **B48**, 5230 (1993).
[12] J. B. Krieger and G. J. Iafrate, Phys. Rev. **B35**, 9644 (1987).